Experimental hydroelastic responses of an elastic container ship-inspired barge model produced using additive manufacturing

Grammatikopoulos, A.[1] , Banks, J.[2] and Temarel, P.[3*]

Fluid-Structure Interactions Group, University of Southampton
[1]Email: ag3e15@soton.ac.uk
[2]Email: J.Banks@soton.ac.uk
[3]Email: P.Temarel@soton.ac.uk

ABSTRACT

Despite significant advancements in the field of computational hydroelasticity, manufacturing methods for corresponding physical models have not changed beyond the flexible backbone concept in the past 20 years. Few researchers have attempted to produce continuous models with an accurate internal structure, the so-called elastic models, in order to obtain more detailed measurements of the structural responses. These investigations faced the limitations of the then available manufacturing methods, which did not allow for any internal details of the structure, apart from bulkheads, to be included in the design without significant increase in difficulty and cost. The resulting structures, although continuous, comprised of an external shell and the effects of cross-sectional shape could not be investigated.
In this investigation, manufacturing difficulties of the past are overcome by use of additive manufacturing to create a barge model with a container ship-inspired cross section. The design and manufacturing processes are presented, followed by vibration tests and towing tank tests in regular head waves. The measured vertical bending moment responses in various stations were found to correlate well with 2D hydroelasticity and the strain distribution along the cross section of the vessel indicated beam-like behaviour. A detailed discussion of the challenges and sources of uncertainty is included, along with suggestions for future work.

Keywords: Elastic model; Additive manufacturing; Container ship; Barge; Vertical bending

1. INTRODUCTION

While hydroelastic analyses have come a long way in the past 20 years, design and production processes for the corresponding experimental models have not changed significantly from the flexible backbone concept. Computational methods to model the effects of hydroelasticity have gradually evolved from 2D (Bishop and Price, 1979) to fully 3-dimensional codes,

*Correspondence to ag3e15@soton.ac.uk

either using potential flow methods (Kim et al., 2015) or computational fluid dynamics (Lakshmynarayanana et al., 2015). For the former, the hydrodynamic codes are coupled with finite element models, which can also be 3-dimensional (Hirdaris et al., 2003), to produce a coupled hydroelastic formulation.

On the other hand, it is common practice for models to be produced with the hydrodynamic and structural aspects segregated. The hull form is produced by slicing a conventional model into rigid segments. The appropriate stiffness is then introduced by means of either a flexible backbone (Peng et al., 2014) or a series of flexible joints (Lavroff et al., 2007). The design process is based on beam approximation and scaling of at least the two-node bending natural frequency. Bending stiffness distribution is, more often than not, ignored for manufacturing simplicity; few exceptions include the work by Dessi and Mariani (2008) who manufactured a non-uniform backbone depicting the bending stiffness distribution of a fast ferry. Use of flexible joints allows for easy tuning of the stiffness and its distribution (Wu et al., 2003). However, the structural properties are not modelled for a continuous structure, which can be considered a relative advantage of the backbone models. Even in the case of the latter, the cross sectional shape and shear area of the actual ship structure are ignored and only the 2nd moment of area is modelled. When investigations focus on the antisymmetric hydroelastic responses of the vessel, coupling between horizontal bending and twisting is usually provided by use of a U-shaped backbone (Kim et al., 2014) or a standard box-shaped one with deck openings cut into it (Zhu et al., 2011).

A number of investigations used continuous models with elastic material, to produce a more detailed structure, the so-called elastic models, in order to counteract the aforementioned issues as well as seek a more detailed structural response. Both Watanabe et al. (1989) and Chen et al. (2001) manufactured elastic models of the S175 container ship. The vessel was first introduced in the 15th and 16th International Towing Tank Conferences (ITTC) as a joint experimental and computational project involving several institutions for a comparative study of hydrodynamic and structural loads. While deflections were measured directly on the structure of these continuous models, their cross section did not resemble that of the full-scale vessel (Wu et al., 2003), with ensuing issues related to shear deflection, torsion of cellular structures etc. However, manufacturing limitations would otherwise render production almost impossibly complicated. Consequently, researchers were discouraged from using elastic models more extensively.

In this paper, additive manufacturing is proposed as a means to overcome the production difficulties faced in the past. Current technology allows for complex cross sections to be produced, with the end result closer to a real ship. A rectangular barge with a constant, container ship-inspired, cross section was produced using ABS, its main particulars approximately corresponding to a scaled-down version of the S175. The simple external geometry was selected to focus on structural issues. The barge was manufactured in segments, joined using solvents. Deep frames, transverse bulkheads and 16 strain gauges were installed throughout the vessel. Tests in regular waves are compared to 2D hydroelasticity predictions for verification. Hammer tests provide further understanding of the dynamic behaviour. Limitations of the method, mainly relating to material and manufacturing constraints and uncertainties are discussed together with possible solutions.

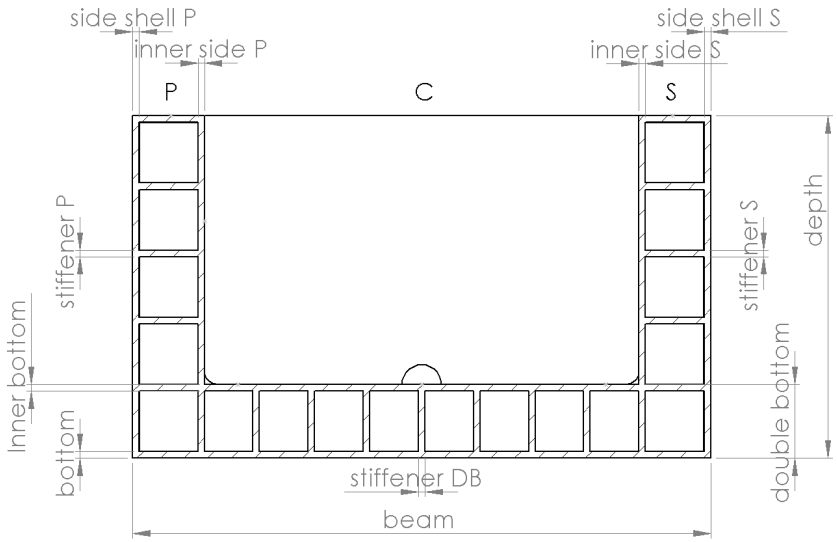

Figure 1: Cross section the uniform barge illustrating measurements taken to evaluate manufacturing uncertainties.

2. METHODOLOGY

2.1. Model design, production and instrumentation

The model produced for the purposes of this investigation was based on the S175 container ship. The scales previously used by Wu et al. (2003) and Watanabe et al. (1989) would result in a model too large for its cross section to fit in a conventional 3D printer. It was considered essential to avoid joining within the cross section as this would introduce additional uncertainties. As a result, the model was scaled down further to overcome this obstacle, with principal dimensions scaled uniformly. The model was designed with a uniform cross section (see Figure 1), for manufacturing simplicity purposes but also to allow for an easy first estimation of the EI needed to achieve the desired 2-node bending natural frequency.

It was decided to scale the displacement of the vessel rather than the draft, as the former would be more relevant to the dynamic properties and natural frequency. Consequently, the draft was smaller than if directly scaled, as the new model was barge-shaped. It should be emphasised, however, that the aim of this investigation was not to produce a scaled-down version of the S175 but rather a vessel with similar characteristics, allowing for qualitative comparison. A summary of the particulars of the vessel is shown in Table 1.

The walls of the model, shown in Figure 1, were designed with a thickness of 2.5 mm but were ultimately thicker (average thickness of 2.91 mm with a standard deviation of 0.12 mm) due to the thickness being close to the printer's limits of manufacturing accuracy. The 2nd moment of area of the cross section as per design would be equal to 5.2E-06 m^4. However, when calculated based on thickness measurements throughout the vessel, the average 2nd moment of area was found to be equal to 6.1E-06 m^4. The bending stiffness was predicted by combining the latter with with flexural modulus values obtained from 3-point bending tests of 3D-printed ABS coupons (average of 1124.69 MPa, with a standard deviation of 64.70 MPa). Using this bending stiffness and the non-uniform mass distribution in a non-uniform beam model (effective shear area equal to 1/3 of the cross-sectional area), the expected in vacuo 2-node bending natural frequency was found to be equal to 40 Hz. It was thus known, even before production had started, that the model would be stiffer than a scaled-down version of the S175, the natural

Table 1: Principal particulars of the cellular barge. The dry and wet 2-node bending natural frequencies are as measured from vibratory (hammer) tests, on the model and the EI derived from the measured dry natural frequency.

Dimension	Symbol	Value
Length between perpendiculars (m)	L	1.520
Beam (m)	B	0.220
Depth (m)	D	0.130
Draft (m)	T	0.047
Displacement (kg)	Δ	15.88
Block Coefficient	C_B	1.00
Bending stiffness (Nm^2)	EI	12078
Natural frequency in vacuo (Hz)	$f_{2\text{-node, vacuo}}$	53.0
Natural frequency in water (Hz)	$f_{2\text{-node, water}}$	31.0

frequency of which would have been 19 Hz in vacuo. As shown in Table 1, the measured 2-node bending natural frequency of the vessel in vacuo was found to be 53 Hz, for reasons that will be discussed in Section 3.

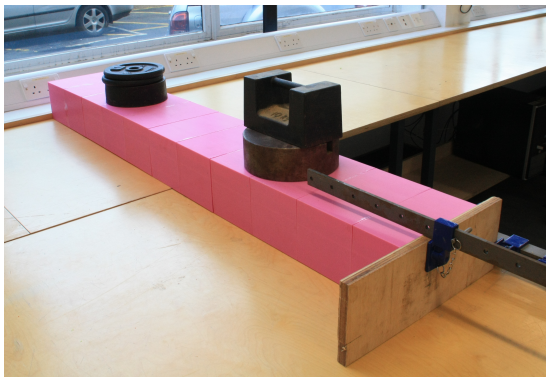

(a) Section joining

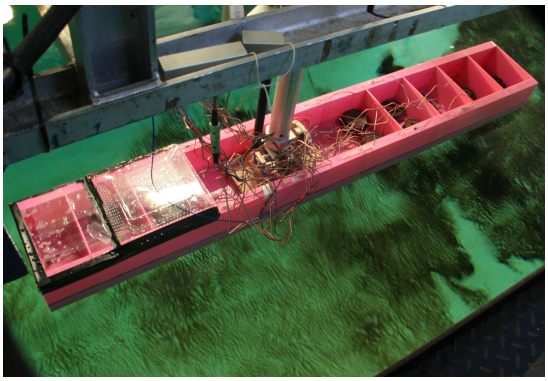

(b) Model in towing tank

Figure 2: Joining of the sections using ABS solution as adhesive and sash clamps as a constraint (a) and fully instrumented cellular barge model in the towing tank (b).

The model was made up of 11 sections, 10 sections of 140 mm length and the foremost section of 120 mm length to achieve the scaled length of the S175. All sections featured a deep frame at one end, namely the aft end. The sections were joined using a solution of the printing material (ABS) in acetone. The sections were constrained together using sash clamps while the acetone was evaporating to leave just ABS in the area of connection (Figure 2a). The vessel was then sanded using a power sander and coated with clear acrylic paint to improve resistance to water absorption. Bulkheads (4 mm thickn) were fitted on all deep frame locations, apart for the ones around the area of the tow post. The sections and bulkheads were produced using an UP Box printer and ABS filament, at a layer height of 0.25 mm.

16 strain gauges were installed, post 3D printing, in various locations of the hull: 5 on Main deck Port side, 3 on Main deck Starboard side, 5 on double bottom Centreline and, finally, an additional 3 strain gauges amidships, two near either corner of the double bottom and one on the inner side. Details of the locations of the strain gauges are shown in Table 2 and Figure 3. The strain gauges used were Micro-Measurements C2A-06-250LW-350 linear quarter-bridge strain gauges with a resistance of 350 Ω and a gauge factor of 2.150$\pm$0.5%.

Table 2: Positioning of strain gauges

#	Station	Transverse location	Vertical location
0	15.0	Port	Main Deck
1	12.5	Port	Main deck
2	10.0	Port	Main deck
3	7.5	Port	Main deck
4	5.0	Port	Main deck
5	15.0	Starboard	Main deck
6	10.0	Starboard	Main deck
7	7.5	Starboard	Main deck
8	15.0	Centreline	Inner bottom
9	12.5	Centreline	Inner bottom
10	10.0	Centreline	Inner bottom
11	7.5	Centreline	Inner bottom
12	5.0	Centreline	Inner bottom
13	10.0	Port	Inner side
14	10.0	Port	Inner bottom
15	10.0	Starboard	Inner bottom

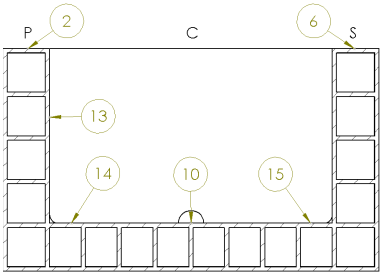

Figure 3: Locations of strain gauges amidships (i.e. Station 10.0). Main deck and Inner bottom locations same for other Stations (See also Table 2).

2.2. Static, modal & towing tank testing

The vessel was subjected to static tests to calibrate the sensors and identify the coefficients required to convert measured strains to bending moments. This calibration was carried out by incrementally increasing a weight applied on the unballasted simply supported hull in vacuo, resulting in the following conversion equation (Roark et al., 1976).

$$M = \frac{P(L-l_P)x}{L} - P\langle x - l_P\rangle \tag{1}$$

where M is the bending moment at location x for a simply supported beam of total length L when a vertical point load P is applied at location l_P. In this manner, the strains were converted to bending moments directly and without the need to assume an EI for the model.

The vessel was also subjected to modal analysis testing to identify its natural frequencies. The dynamic flexural modulus was derived from the 2-node bending natural frequency in vacuo. For the in vacuo modal analysis, the model was suspended using flexible bungee cords at the nodal locations of the 2-node bending mode, to minimise the influence of support on the aforementioned mode (Carne et al., 2007). The roving hammer setup used a PCB-086C03 instrumented hammer (sensitivity: ($\pm$15%) 2.25 mV/N) for the excitation measurement and a PCB-352C33 accelerometer (sensitivity: ($\pm$10%) 10.2 mV/m/s^2), located amidships (1cm off centreline to port), for the response measurement. Both measurements were obtained using a DataPhysics Quattro Dynamic Signal Analyzer and SignalCalc software and the latter was also used for the calculation of the relevant frequency response functions.

Measurements in both static (sensor calibration) and towing tank tests were obtained using a National Instruments cDAQ-9135 Data Logger and two National Instruments NI-9236 strain gauge modules. During towing tank tests, heave and pitch were measured using the tow post dynamometer and transferred from the amplifying unit to a NI-9205 Voltage module. All the above measurements were obtained using LabVIEW software. The wave probe measurements

during the tank tests were obtained through the Lasso software, developed by the Wolfson Unit.

The stationary model was tested in regular head waves in the Solent University towing tank (60m x 3.7m x 1.8m). The tow post was placed at Station 12, i.e. 10% forward of the midship section. A piece of plywood 250 mm long and 150 mm wide, connected to the model using captive nuts and threaded bars served as the base for the tow post (as shown in Figure 2b). The ballast distribution was designed to achieve an even-keel vessel.

Table 3: Wave/ship length ratios and frequencies for the tests in regular waves. A wave height of 0.05 m was used in all cases.

λ/L	ω (rad/s)	f (Hz)
0.6	8.22	1.31
0.8	7.12	1.13
0.9	6.71	1.07
1.0	6.37	1.01
1.1	6.07	0.97
1.2	5.81	0.93
1.3	5.59	0.89
2.0	4.50	0.72

The height of the regular waves was kept constant at 0.05 m, corresponding to H_{wave}/L_{BP} of 1/30. The wave frequencies were selected based on the λ/L used by Chen et al. (2001) and Wu et al. (2003) for the relevant wave height ratio (see Table 3). Each test condition was repeated three times.

A 2D hydroelasticity code based on linear strip theory and linear Timoshenko beam theory was used for comparison (Bishop and Price, 1979). The ship was divided into 50 sections along the length and the non-uniform mass was accounted for. A shear area coefficient of 1/3 was used, a selection based on experience. The flexural modulus used in this analysis was evaluated from the in vacuo 2-node bending natural frequency obtained from the vibratory tests.

3. RESULTS AND DISCUSSION OF UNCERTAINTIES

An iterative process, in conjunction with Timoshenko beam theory, is used, whereby the value of the flexural modulus E is varied until the in vacuo 2-node bending natural frequency matches the one from vibratory tests, namely 53 Hz. This iterative process results in E equal to 1.98 GPa. Thus it can be seen that the 2-node bending natural frequency of the vessel was under-predicted during the design stage (predicted natural frequency based on 3-point bending tests was 40 Hz). As the geometric characteristics of the vessel and the mass distribution were known with good accuracy, the discrepancy was attributed to a difference in the flexural modulus of the vessel compared with that obtained from 3-point bending tests of coupons.

Differences in the flexural modulus found by the 3-point bending tests could be attributed to two distinct causes. Firstly, the standardised coupon thickness used in the tests was higher than that of the vessel itself. As the thickness was reduced from 4 mm for the coupons to 2.5 mm for the vessel (wall thickness), the part of the wall that comprised the infill was reduced and, at the same time, printing close to the operational limits (minimum printable thickness) of the printer increased overlap of the infill. This resulted in an almost entirely solid cross section, which was bound to have a higher E than a specimen in which the modulus is calculated as an average over a cross section containing air gaps. A second cause of discrepancy was the fact that the flexural

modulus for polymers in dynamic conditions can be different than the static one. Indeed, an extensive study on the vibratory properties of 3D printed components (Grammatikopoulos et al., 2018) identified a dynamic flexural modulus which was significantly higher than the one predicted by 3-point bending. Specimens in this study comprised thin-walled rectangular cells of the same material and the predicted dynamic flexural modulus was 2.11 GPa.

Static tests (sensor calibration) revealed an apparent local increase of stiffness around the area of the tow post. The sensor primarily affected was strain gauge 9, which is located underneath the plywood piece, at Station 12.5. This locally increased stiffness was observed both in the static and dynamic responses of the vessel.

Responses in heave and pitch are shown in Figure 4, whereas bending moment responses are shown in Figure 5. The latter were based on strain measurements on the main deck of the vessel, Port side, on five Stations (5.0, 7.5, 10.0, 12.5 and 15.0). The strains were converted to bending moments using the bending moment/strain coefficients obtained from the static tests. The bending moments from the strain measurements and the 2D hydroelasticity predictions were then non-dimensionalised using the following equation:

$$C_M = \frac{M}{\rho g L^2 B A_{wave}} \tag{2}$$

where M is the bending moment, ρ is the water density, L and B are the length and beam of the vessel, respectively and A_{wave} is the wave amplitude.

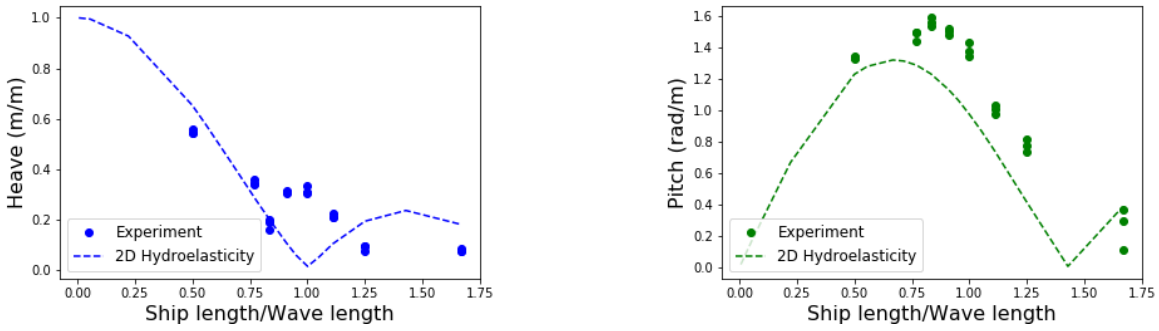

(a) Heave response

(b) Pitch response

Figure 4: Heave and pitch RAOs of the uniform barge.

Good agreement is observed between 2D Hydroelasticity and experimental measurements. Discrepancies between measured & predicted rigid body motion responses may be attributed to the use of Lewis sections for a vessel with rectangular cross sections and vertical bow and stern walls. Peak bending moment responses were measured, as would be expected, at the wave-ship matching region; bottom slamming was also observed in this region, particularly for λ/L equal to 1.0. Bending moments measurements were found to have slightly better agreement with 2D hydroelasticity for the aft half of the vessel (Stations 5.0, 7.5 and 10.0). Measurements were found to be less consistent between runs for shorter wave lengths and differences between measurements and 2D hydroelasticity predictions also increased for these cases. Green water was observed on the deck of the vessel for these higher frequencies, particularly during tests at λ/L=0.6. The bluff bow of the vessel would crash into these shorter waves and part of the wave would run over the fore deck. Overall, looking at the non-dimensionalised vertical bending moment coefficients, it was observed that the first harmonic component had similar values as

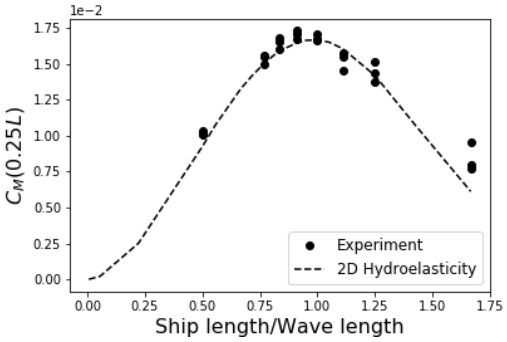

(a) Station 5

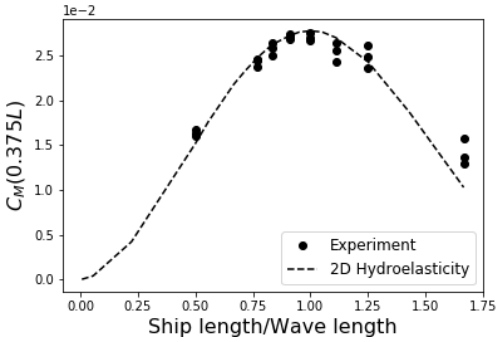

(b) Station 7.5

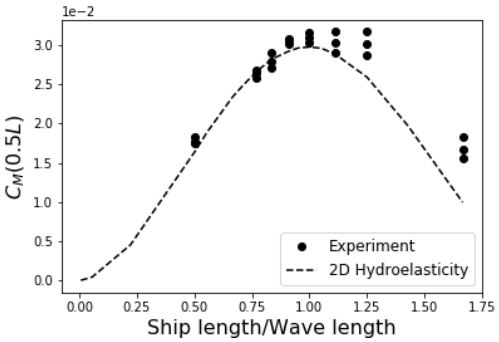

(c) Station 10

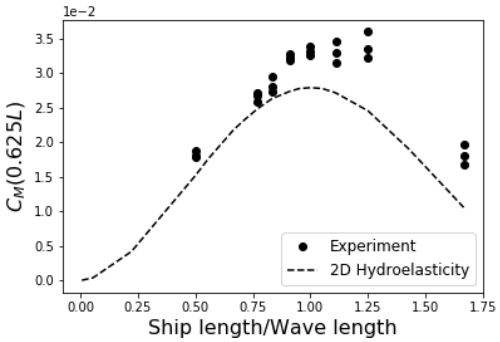

(d) Station 12.5

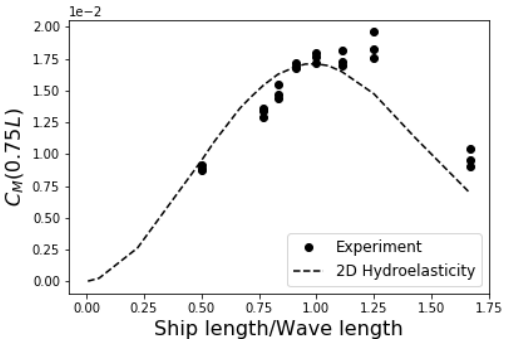

(e) Station 15.0

Figure 5: Bending moment measurements along the length of the vessel, based on strain measurements on Main deck Port side. 2D hydroelasticity results (based on linear strip theory and linear beam theory) are also presented for comparison. The loads were non-dimensionalised based on Eq. 2.

the ones measured by Chen et al. (2001) and the magnitude ratios between the first, second and third harmonics also featured comparable trends, as can be seen in Figure 6a.

As the 2-node bending natural frequency of the vessel was not even remotely close to the wave frequency range under investigation, no resonant behaviour due to linear springing was observed. Looking at a typical strain response in Figure 6a, a peak corresponding to the wet 2-node bending natural frequency is clearly visible at 31 Hz, caused by vessel slamming and consequent whipping responses, although these did not dominate the strain measurements. The amidships strain distribution from deck to bottom, shown in Figure 6b, is fairly linear, agreeing with beam theory.

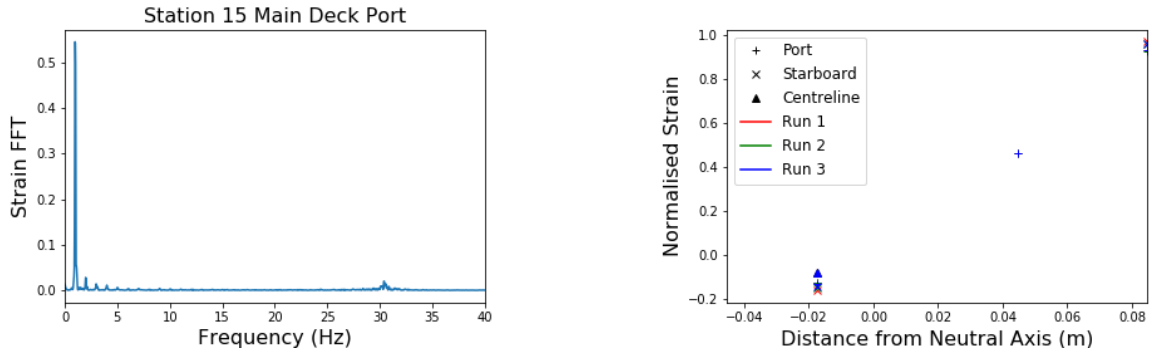

(a) Strain FFT

(b) Strain distribution

Figure 6: (a) Frequency content of the strain response in regular head waves at an excitation frequency of 1.01 Hz (λ/L=1.0) (b) Strain distribution throughout he midship section for the same excitation frequency.

4. CONCLUSION

In this investigation, an elastic ship model with a detailed cross section was designed, produced and tested for the first time. The vessel design was inspired by the S175 container ship particulars combined with the cross-sectional geometry of a realistic container ship. The vessel was subjected to static tests for calibration of the 16 strain gauges, vibration tests to determine its modal properties and, finally, towing tank tests in regular head waves at zero forward speed for a range of frequencies.

The qualitative, as well as quantitative, analysis of wave-induced motions and loads was verified using 2D hydroelasticity theory predictions. The bending moment RAO magnitudes are in line with those measured by Chen et al. (2001) for the S175 container ship. Furthermore, the frequency content of the strain (or bending moment) spectra show similar comparative magnitudes between first, second and third harmonic components as per Chen et al. (2001). These are all significant indicators for the validity of the model concept reported in this paper. It should also be noted that the uniform barge with cellular cross-sectional structure does behave as a Timoshenko beam.

The discrepancies observed for the rigid body motions can be attributed to the limitations of the applied method for bluff bodies. Unlike rigid and flexible backbone models, elastic models require careful consideration with reference to the attachment of the tow post. The recommendation is to aim for as reduced a footprint as possible. With the current tow post arrangement, it is important to model the local stiffening effects, which limits the applicability of beam-type idealisation and would require a 3D finite element model of the structure.

The additive manufacturing process introduced uncertainties in manufacturing tolerances which were particularly visible in the wall thickness of the model. Nevertheless, advances in the relevant hardware technology are rapidly improving these tolerances. The most important issue is the prediction of the dynamic flexural modulus of 3D printed polymers, such as ABS, which is essential in calculating the bending stiffness and corresponding 2-node natural frequency of the model. 3-point bending coupon tests of 3D printed polymer coupons, provide underestimated predictions for the dynamic flexural modulus of the structure in question. Further work on this subject indicated that a method involving vibration testing of specimens with a thin-walled cellular beam geometry provides an accurate prediction of the flexural modulus (Grammatikopoulos et al., 2018). Furthermore, as was previously discussed, the flexural

modulus for 3D printed polymer components can be quite different between static and dynamic loading conditions. It can be, thus, argued that converting strains to bending moments by use of static tests potentially introduces additional uncertainties.

ACKNOWLEDGEMENTS

The present investigation was funded by the Lloyds Register Foundation University Technology Center on Ship Design for Enhanced Environmental Performance.

REFERENCES

Bishop, R. E. D. and Price, W. (1979). *Hydroelasticity of ships*. Cambridge University Press.

Carne, T. G., Griffith, D. T., and Cassias, M. E. (2007). Support Conditions for Free Boundary-Condition Modal Testing. *IMAC-XXV: A Conference & Exposition on Structural Dynamics*, (January 2015).

Chen, R.-Z., Du, S.-X., Wu, Y.-S., Lin, J.-R., Hu, J.-J., and Yue, Y.-L. (2001). Experiment on extreme wave loads of a flexible ship model. In *Practical Design of Ships and Other Floating Structures. Proceedings of the Eighth International Symposium on Practical Design of Ships and Other Floating Structures*, volume 2, pages 871–878.

Dessi, D. and Mariani, R. (2008). Analysis and Prediction of Slamming-Induced Loads of a High-Speed Monohull in Regular Waves. *Journal of Ship Research*, 52(1):71–86.

Grammatikopoulos, A., Banks, J., and Temarel, P. (2018). Experimental dynamic properties of ABS cellular beams produced using additive manufacturing. In *ECCM18 - 18th European Conference on Composite Materials*, Athens, Greece.

Hirdaris, S. E., Price, G. W., and Temarel, P. (2003). Two- and three-dimensional hydroelastic modelling of a bulker in regular waves. *Marine Structures*, 16(8):627–658.

Kim, B. W., Kim, K.-H., Kim, Y. S., and Hong, S. Y. (2014). Torsion Moment Conversion Methods in Model Test With U-shape Backbone. 3:782–791.

Kim, J. H., Kim, Y., Yuck, R. H., and Lee, D. Y. (2015). Comparison of slamming and whipping loads by fully coupled hydroelastic analysis and experimental measurement. *Journal of Fluids and Structures*, 52:145–165.

Lakshmynarayanana, P., Temarel, P., and Chen, Z. (2015). Hydroelastic analysis of flexible barge in regular waves using coupled CFD-FEM modelling. *Marstruct-2015*, pages 95–103.

Lavroff, J., Davis, M. R., Holloway, D. S., and Thomas, G. A. (2007). The Whipping Vibratory Response of a Hydroelastic Segmented Catamaran Model. In *Ninth International Conference on Fast Sea Transportation*, Shanhai, China.

Peng, S., Temarel, P., Bennett, S. S., Wu, W., Liu, Z., and Wang, Y. (2014). Symmetric response of a hydroelastic scaled container ship in regular and irregular waves. In *Proceedings of the ASME 2014 33rd International Conference on Ocean, Offshore and Arctic Engineering OMAE2014*, pages 1–10, San Francisco, California, USA. ASME.

Roark, R. J., Young, W. C., and Plunkett, R. (1976). *Formulas for Stress and Strain*, volume 43.

Watanabe, I., Ueno, M., and Sawada, H. (1989). Effects of Bow Flare Shape to the Wave Loads of a container ship. *Journal of the Society of Naval Architects of Japan*, 1989(166):259–266.

Wu, Y.-S., Chen, R.-Z., and Lin, J.-R. (2003). Experimental technique of hydroelastic ship model. In *Proceedings of the Third International Conference on Hydroelasticity, Oxford, UK, September*, pages 15–17.

Zhu, S., Wu, M., and Moan, T. (2011). Experimental investigation of hull girder vibrations of a flexible backbone model in bending and torsion. *Applied Ocean Research*, 33(4):252–274.